Nenad Gubeljak[1], JožePredan[1], Inoslav Rak[1], Dražan Kozak[2]

INTEGRITY ASSESSMENT OF HSLA STEEL WELDED JOINT WITH MIS-MATCHED STRENGTH

OCENA INTEGRITETA ZAVARENOG SPOJA HSLA ČELIKA RAZLIČITE ČVRSTOĆE OSNOVNOG METALA I METALA ŠAVA

Author's address:
[1] University of Maribor, Faculty of Mechanical
Engineering Maribor, Slovenia nenad.gubeljak@uni-mb.si
[2] University of Osijek, Mechanical Engineering Faculty in
Slavonski Brod, Croatia

Keywords
- HSLA steel
- welded joint
- mis-matching
- base metal
- weld metal
- stress intensity factor
- crack opening displacement
- structural integrity assessment

Ključne reči
- HSLA čelik
- zavareni spoj
- mismečing
- osnovni metal
- metal šava
- faktor intenziteta napona
- otvaranje prsline
- ocena integriteta konstrukcije

Abstract

Currently, there is a need to conduct numbers of validation cases for the defect assessment procedure of the recently developed Structural Integrity Assessment Procedure (SINTAP). Current work deals with the application of SINTAP mis-match (Level II) option to the high strength low alloy (HSLA) steel multi-pass weldment. The fracture behaviour was estimated using CTOD bend specimens with surface and through thickness notches in the middle of X-groove weld metal. The effects of strength mis-match (M) between base and weld metals and the weld width (2H) should be taken into account in the mis-match option of the SINTAP procedure, if M > 1.1. The SINTAP procedure uses the minimum width of the weld metal for through thickness and surface cracked configurations to calculate the limit loads. The surface cracked bend configuration needs to be treated in more detail for the validation of the SINTAP procedure. Application of the SINTAP procedure has been performed by analysing the predicted and experimentally obtained crack initiation load for stable crack growth and determining the load carrying capacities of the bend bars.

Izvod

Aktuelna je potreba da se na nizu slučajeva pokaže važenje procedure za ocenu grešaka prema nedavno razvijenoj „Proceduri za ocenu integriteta konstrukcija" (SINTAP). U ovom članku se razmatra primena opcije SINTAP mismečing (nivo II) na višeprolazni zavareni spoj niskolegiranog čelika visoke čvrstoće (HSLA). Ponašanje pri lomu je određeno korišćenjem CTOD epruveta za savijanje sa površinskim i prolaznim zarezom u sredini metala šava izvedenog u X žlebu. Uticaj mismečinga (M) u čvrstoći osnovnog metala i metala šava i širine šava (2H) treba uzeti u obzir u mismečing opciji procedure SINTAP, ako je M > 1,1. U proceduri SINTAP se pri proračunu graničnog opterećenja koristi minimalna širina metala šava oblika sa prolaznom i površinskom prslinom. Konfiguraciju sa površinskom prslinom za savijanje treba mnogo detaljnije razmatrati pri oceni procedurom SINTAP. Procedura SINTAP je sprovedena analizom predviđenih i eksperimentalno dobijenih početnih opterećenja za stabilni rast prsline i određivanjem veličine opterećenja koje može preneti štap opterećen na savijanje.

INTRODUCTION

Reliable assessment of the structural integrity of high strength steel mis-matched welds has an important role for safe use of welded structure. To ensure overmatched weld metal (WM) and good weldability, the consumable material of low level content of carbon and alloying additions was used /1/. Usually, such consumables produce heterogeneous microstructure of weld metal in multi-pass welded joints. Consequently, the mechanical properties vary with micro-

structure through the welded joint thickness. The resulting differences in mechanical properties through the welded joint affect the accuracy of input data in different procedures, such as R6 /2/, EPRI /3/, WES /4/, Engineering Treatment Model (ETM-MM) /5/, SINTAP /6/. The accuracy of input data is important for results of prediction model.

The aim of this article is to assess the integrity of mismatched welded joints of high strength steel using SINTAP

procedure and single notched three point bend specimens (SENB). The performed assessment was done with both through the thickness and surface crack with the tip positioned in the middle of the weld metal. In the specimen with the surface crack, the tip can be located almost in one microstructure along the weld pass, but in the specimen with the through-the-thickness crack, the tip is located in all microstructures of the weld metal. To assess the significance of weld defect in a component, the effect of fracture parameter value, stress intensity factor (K_I), or crack tip opening displacement (CTOD) on the load and deformation, is necessary.

WELDING AND MATERIALS PROPERTIES

Investigated steel is NIONICRAL 70A, a low alloyed high strength (HSLA) steel (HT80 class). Different mechanical properties of this steel can be obtained by different tempering temperatures (600–800°C). The base metal (BM) microstructure consists of tempered martensite and upper bainite, providing both high strength and impact toughness.

Using standard welding procedure specification (WPS), 40 mm thick welded joint was produced with "X" groove (Fig. 1). By applied filler metal, flux cored electrode

$\varnothing$1.2 mm, a strength overmatched weld was produced. The following welding parameters were used: heat input $Q = 20$ kJ/cm, critical cooling time $\Delta t_{8/5} = 8$–12 s, preheating temperature $T_p = 50$–135°C.
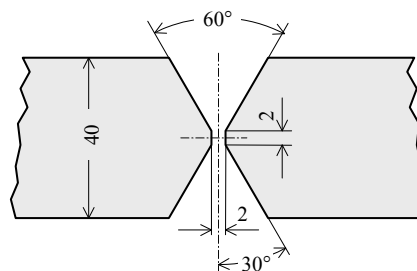

Figure 1. The "X" shaped groove used in this investigation.
Slika 1. Žleb „X" oblika je korišćen u ovom istraživanju

Mechanical properties were determined according to DIN 50125. Standard tensile specimens, 5 mm in diameter, were made from the root and top regions of the welded joint along the welding direction. The average values of tensile properties are given in Table 1.

Table 1. Tensile properties of base and weld metals at −10°C (average values).
Tabela 1. Zatezne karakteristike osnovnog metala i metala šava na −10°C (prosečne vrednosti)

Material	Testing temperature	Elasticity modulus	Yield stress	Tensile strength	Linear elastic limit stress	Strain hardening exponent	Elongation at fracture	Mis-match factor
	t, °C	E, GPa	$R_{P0.2}$, MPa	R_m, MPa	σ_o, MPa	n	A_t, %	M
Base metal	20	201	711	838	679	0.091	19.6	–
	−10	209	712	846	676	0.095	19	–
Weld metal WM$_1$	20	210†	770	845	747	0.065	16	1.08*
Weld metal WM$_{1fill}$	20	205	861	951	833	0.074	11.7	1.21
	−10	211	873	1041	833	0.107	10.8	1.22
Weld metal WM$_{1root}$	20	221	807	905	780	0.075	15.3	1.14
	−10	212	824	902	801	0.064	16.5	1.16

*estimated value, no experimental data available; WM$_{1fill}$–fill passes; WM$_{1root}$–root passes

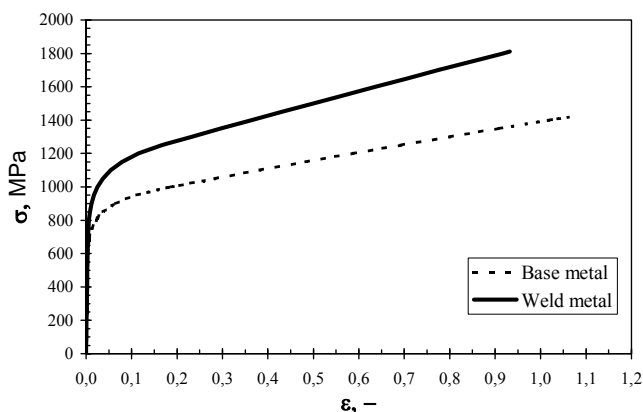Typical true stress-true strain curves are shown in Fig. 2.

Figure 2. Average true stress–true strain curves of weld metal and base metals with visible overmatching.
Slika 2. Prosečne krive stvarni napon–stvarna deformacija metala šava i osnovnog metala sa vidljivim overmečingom

Charpy impact toughness testing of base and weld metals was performed at −10°C and −40°C on standard specimens,

with the "V" notch positioned in WM different regions. The values of impact energy are given in Table 2.

Table 2. Charpy impact energy of base and weld metals Kv, J.
Tabela 2. Energija udara Šarpi osnovnog metala i metala šava Kv,J

Material	Base metal	WM$_1$	WM$_{1fill}$	WM$_{1root}$
−10°C	85	56	56	61
−40°C	54		33	50

The average curves for impact toughness vs. temperature in three WM regions are shown in Fig. 3. It is clear that local brittle zones (LBZ) are less concentrated at the weld surface than in the weld root.

Strength mismatching factor M is defined as the ratio of yield strength of WM, $R_{p0.2, WM}$ and that of BM, $R_{p0.2, BM}$:

$$M = \frac{R_{p0.2,WM}}{R_{p0.2,BM}} \tag{1}$$

The obtained values for the strength mismatching factor M differ from designed value (Table 1), due to metallurgical processes during welding and alloying of WM by dilution of BM l, depending on the heat input and travel speed.

In addition, Vickers hardness measurement was conducted in the weld thickness direction with indentation spacing 0.25 mm, Fig. 4. Since the mechanical properties shown in Table 1 represent average values of the regions where specimens were taken from, they cannot provide the exact mis-matching factor value valid for the weld as a whole. The microhardness in the multi-pass welded joint can indicate strengths variation caused by microstructure.
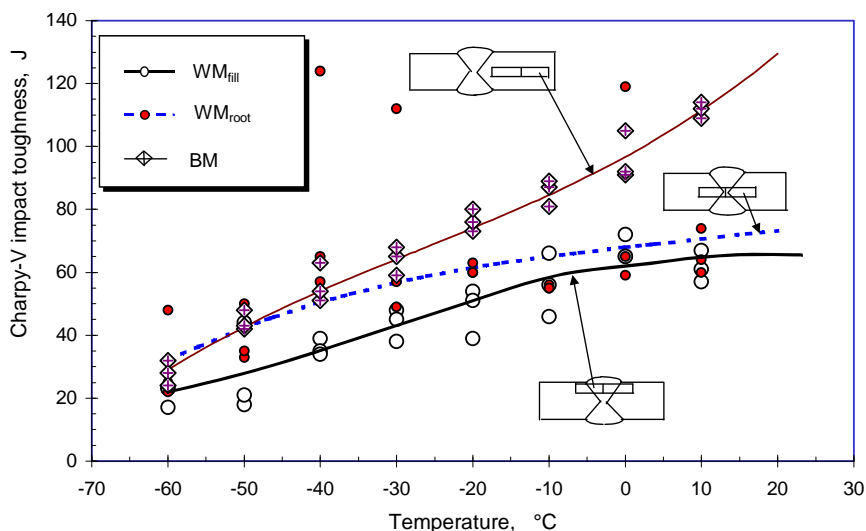

Figure 3. Average impact toughness vs. temperature curves for different weld metal regions.
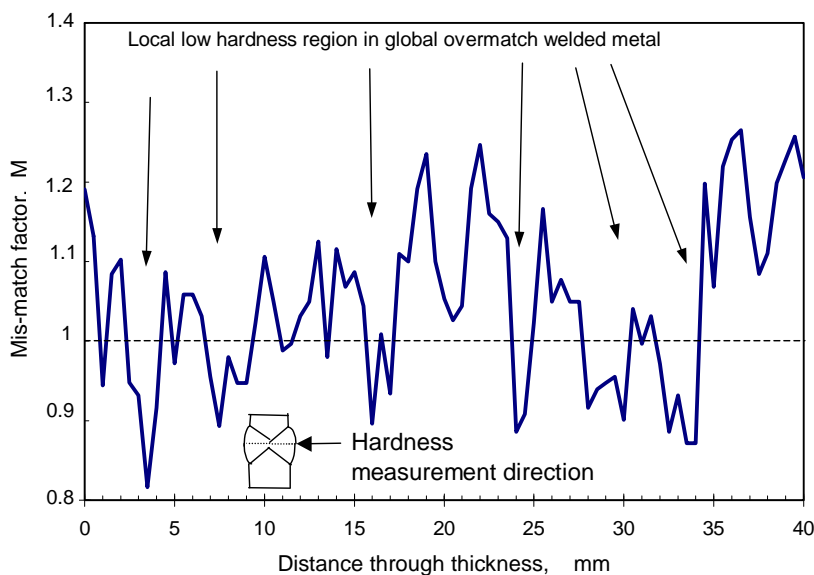Slika 3. Prosečne krive zavisnosti udarne žilavosti od temperature za različita područja metala šava

Figure 4. Distribution of microhardness through-the-thickness section of the welded joint.
Slika 4. Raspodela mikrotvrdoće kroz poprečni presek po debljini zavarenog spoja

FRACTURE TOUGHNESS TESTING OF CRACK TIP OPENING DISPLACEMENT

Three point bend specimens are used for CTOD testing, with notch positions as shown in Fig. 5. The fatigue pre-crack was located on the weld symmetry line. For the through the thickness specimens (B×2B), the pre-cracking was done by modified SHR ("Step high ratio") fatigue procedure /7/ as recommended in BS 7448: Part 2: 1997 /8/.

The CTOD was determined using the direct CTOD (δ_5) measurement method, /9/. The testing temperature of –10°C was chosen in accordance with the recommendations of the International Society for "Offshore Mechanics and Arctic Engineering – OMAE" /10/. The single specimen technique was used, with crack length measurement by the potential drop method, i.e. by Johnson's method, /11/. The loading with stroke rate 0.1 mm/min was displacement controlled.

In all weld metal specimens after initial blunting and a certain amount of stable crack growth, unstable fracture occurred (pop-in), Fig. 6. The achieved values of fracture toughness parameters according to ASTM E 1290-93 /12/ and EFAM-GTP /13/ document are listed in Table 3.

Base metal B×2B specimens with a crack depth ratio $a_0/W = 0.5$ were used for testing. For base metal specimens the crack tip opening displacement value δ_{5m} was reached. (δ_{5m} had a value of δ_5 at the maximum sustained force F_{max} during the CTOD test).
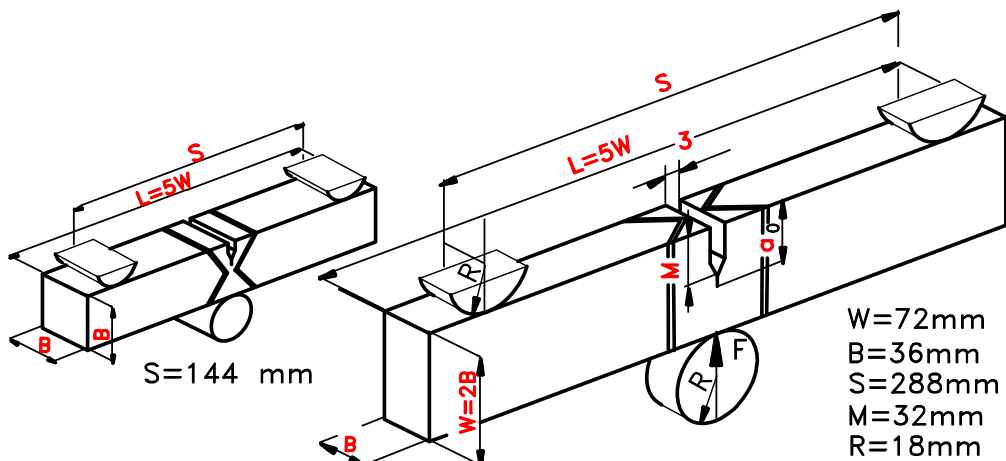
Figure 5. CTOD single edge notch bend specimen.
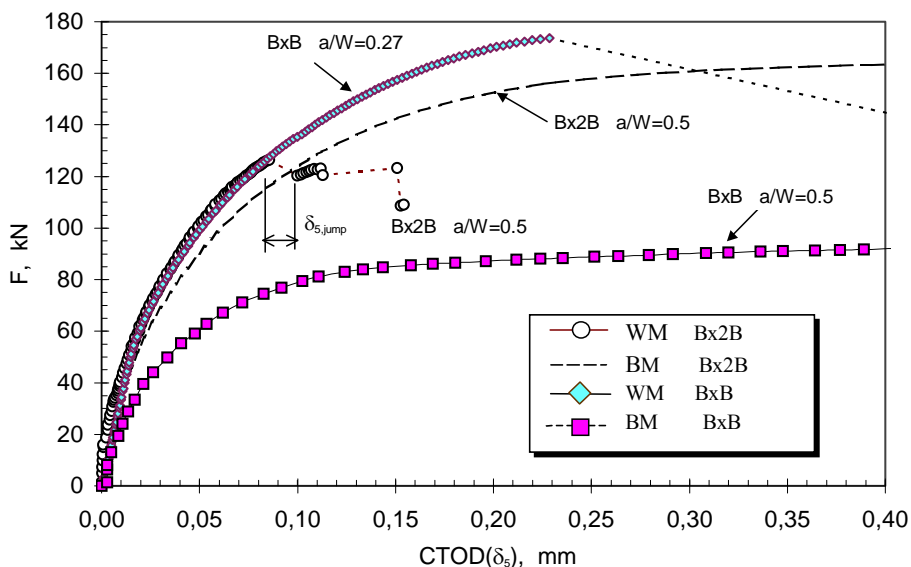Slika 5. CTOD epruveta za savijanje sa jednim bočnim zarezom

W=72mm
B=36mm
S=288mm
M=32mm
R=18mm

S=144 mm

Figure 6. Experimental curves CTOD(δ_5) vs. load F
Slika 6. Eksperimentalne krive zavisnosti CTOD(δ_5) i sile F

Table 3. Fracture toughness parameters values of weld metal according to ASTM E 1290-93 and EFAM-GTP 94.
Tabela 3. Veličine parametara žilavosti loma metala šava prema ASTM E 1290-93 i EFAM-GTP 94

Specimen		Initial		Values at initiation			Maximum values	
		crack length	crack ratio	Crack tip opening displacement	Load	Stress intensity factor	Crack tip opening displacement	Load
		a_0, mm	a_0/W	δ_i, mm	F_i, kN	K_{Ii}, N/mm$^{1.5}$	$\delta_{c,u,max}$, mm	F_{max}, kN
B×B	AX1	9.626	0.27	0.158	161	4337	0,233	178.2
	AX2	9.912	0.27	0.135	152	4230	0.228	173.6
	AX3	10.20	0.28	0,063	157	4261	0.365	157.8
B×2B	AW1	35.85	0.50	0.104	121	4281	0.118	123.4
	AW2	35.23	0.49	0.065	113	4060	0.123	137.8
	AW3	35.41	0.49	0.066	115	4129	0.085	126.5

SINTAP PROCEDURE FOR OVER-MATCHED WELDED JOINTS

Determination of the input data

Considering the quality of input data and the heterogeneity of the welded joint "Level 2: Mis-match" of SINTAP procedure should be used. According to this procedure, it is necessary to know:

– mechanical properties, from Table 1 ($\sigma_y = \sigma_O$, R_m, σ_f, n);
– geometry of specimen or component (B, W, S, a_0), Fig. 5;
– fracture toughness of material region where the crack tip is located (K_I, Table 2).

Both materials (BM and WM) do not exhibit Lüders strains, therefore it is possible to express the true stress-strain tensile behaviour by Ramberg-Osgood relation:

$$\frac{\varepsilon}{\varepsilon_0} = \frac{\sigma}{\sigma_0} + \alpha\left(\frac{\sigma}{\sigma_0}\right)^n \qquad (2)$$

where σ_0 is the proportional (linear elastic) yield stress; α is a non-dimensional constant; n is the hardening exponent. Proportional yield strain, ε_0, can be determined as

$$\varepsilon_0 = \frac{\sigma_0}{E} \qquad (3)$$

The parameters (σ_0, α, n) in the Ramberg-Osgood law are listed in Table 1. In spite of fact that the weld metal exhibits a scatter in hardness and consequently in mechanical properties, average mechanical properties of the welded metal will be used in the further analysis in order to get an insight in microstructural effect.

Determination of the yielding load

For determination of the yield load it is necessary to consider the relevant width of the welded joints which depends on specimen type, /14/.

For B×B specimens with a surface notch, the relevant width of the weld joint is the current width of the weld metal (Fig. 1, Fig. 5). In this case the relevant welded joint width ($2H$) for a crack of length a_0 is given

$$2H = \left[(W - 2a_0)\tan\alpha + 2H_0\right]\cos\alpha \qquad (4)$$

where α is the half average angle of the welded joint gap (30°); $2H_0$ is the narrowest mid-thickness width of the welded joint ($2H_0 = 5$ mm).

For B×2B specimen (Fig. 5) the relevant width of the welded joint remains constant and is the narrowest mid-thickness width of the welded joint ($2H_0 = 5$ mm).

The yielding loads for normalising are determined for plane strain conditions from EFAM-ETM-MM 96, /15/:

$$F_{YB} = \beta\frac{\sigma_{YB}}{\sqrt{3}}\frac{B(W-a)^2}{S/2} \qquad (5)$$

$$F_{YW} = M \cdot F_{YB}$$

where $\beta = 1.199 + 0.096\left(\dfrac{a}{W}\right)$ for $0.172 < a/W < 1$; M is mis-match factor given by Eq. (1). The subscripts B and W refer to the base and weld metal, respectively.

The mis-matched yield load F_{YM} for Single-Edge-Cracked Plates in Three-Point Bending (for deformation pattern A in EFAM-ETM-MM 96) is given by relations:

$$\frac{F_{YM}}{F_{YB}} = \begin{cases} M & for \quad 0 \le \psi \le \psi_1 \\ A + B\dfrac{\psi_1}{\psi} + C\left(\dfrac{\psi_1}{\psi}\right)^M & for \quad \psi_1 \le \psi \end{cases} \qquad (6)$$

where

$$\psi = \frac{W-a}{H}; \quad \psi_1 = 2\cdot e^{-(M-1)/8}$$

$$A = \frac{M+49}{50}; B = \frac{49(M-1)}{50} - C; C = 0.3(M-1)\cdot\sqrt{M-1}$$

Failure assessment diagram route

In the Failure Assessment Diagram (FAD) approach comparison of the crack driving force and the material's fracture toughness are performed for prediction of the initiation load and load limit.

In FAD route a failure assessment curve (FAC) in FAD space, K_r verse L_r, is described by the Equation:

$$K_r = f(L_r) \qquad (7)$$

To assess the crack initiation and growth, two parameters need to be calculated. The first one is K_r, a measure of the proximity to elastic fracture, which is defined by:

$$K_r = \frac{K(a,F)}{K_{mat}} \qquad (8)$$

where $K(a,F)$ is the stress intensity factor (SIF) of the defective component of interest. For example $K(a,F)$ for SENB three point bend specimens is given by the equation:

$$K(a,F) = \frac{F}{B\sqrt{W}}\cdot f\left(\frac{a}{W}\right) \qquad (9)$$

where a is the crack length; F is the applied load; B is the thickness and W is the width of specimen, and $f(a/W)$ is the stress intensity function for a three point bend specimen.

The value K_{mat} is the fracture toughness of the material region where the crack tip is located. This value is determined experimentally by measuring the parameters (F, v_{lld}) up to the initiation point of stable crack growth. The calculated K_{mat} values are listed in Table 2 for each specimen tested.

$$f(\frac{a}{W}) = \frac{3\sqrt{\dfrac{a}{W}}}{2\left(1 + 2\dfrac{a}{W}\right)\cdot\left(1 - \dfrac{a}{W}\right)^{1.5}} \times$$

$$\times\frac{S}{W}\left[1.99 - \frac{a}{W}\left(1 - \frac{a}{W}\right)\cdot\left(2.15 - 3.93\frac{a}{W} + 2.7\left(\frac{a}{W}\right)^2\right)\right] \qquad (10)$$

The second parameter L_r is a measure of the proximity to plastic collapse:

$$L_r = \frac{F}{F_{YM}} \qquad (11)$$

where F is the applied primary load; F_{YM} is the plastic yield load of SENB bend mis-matched specimen, Eq. (6).

Having calculated K_r and L_r, the point (L_r, K_r) is plotted on the FAD graph which is bounded by the FAC, described by Eq. (7) and a cut-off $L_r = L_r^{max}$.

The cut-off L_r^{max} can be determined from:

$$L_r^{max} = \frac{1}{2}\left(1 + \frac{0.3}{0.3N_M}\right) \qquad (12)$$

In Eq.(12) the strain hardening exponent for the mis-matched component, N_M, is estimated from

$$N_M = \frac{(M-1)}{(F_{YM}/F_{YB}-1)N_W + (M - F_{YM}/F_{YB})/N_B} \tag{13}$$

The hardening exponents for the weld metal, N_W, and for base metal, N_B, are estimated from

$$N_W = 0.3\left(1 - \frac{R_{mW}}{R_{p0.2W}}\right); \quad N_B = 0.3\left(1 - \frac{R_{mW}}{R_{p0.2W}}\right) \tag{14}$$

The FAC function $f(L_r)$ is defined in terms of the load ratio $L_r = F/F_Y$ for $0 \le L_r \le L_r^{max}$

$$f(L_r) = \left(1 + \frac{1}{2}L_r^2\right)^{-1/2} \times \left[0.3 + 0.7\,e^{-0.6L_r^6}\right] \tag{15}$$

Crack driving force route

In the crack driving force (CDF) approach the force is plotted and compared directly with the material's fracture toughness, using J-integral or crack tip opening displacement (CTOD). An additional analysis is carried out to determine the plastic limit load. These characterise the state of stresses and strains ahead of the crack tip in a specimen:

$$J = J_e\left[f(L_r)\right]^{-2} \tag{16}$$

where J_e is the elastic value of the J integral which can be deduced from the stress intensity factor K_I as

$$J_e = \frac{K_I^2}{E'} \tag{17}$$

with E' corresponding to the Young's modulus E in plane stress and to $E/(1 - \nu^2)$ in plane strain, where ν is Poisson's ratio. The function $f(Lr)$ is given by Eq. (15).

The parameter J-integral, Eq. (16), can be expressed by CTOD value (δ) by following relationship:

$$\delta = \frac{J}{m \cdot \sigma_{ys}} \tag{18}$$

$$m = -0.111 + 0.817\frac{a}{W} + 1.36R^*; \quad R^* = \left(\frac{500 \cdot n}{2.718}\right)^n \text{ or } R^* = \frac{\sigma_m}{\sigma_y}$$

The terms m and R^* are introduced by Kirk et al, /16/, based on the results of finite element analysis. Substitution of δ from Eq. (18) into Eqs. (16) and (17) produces:

$$\text{CTOD} = \text{CTOD}_e\left[f(L_r)\right]^{-2} \tag{19}$$

with $\text{CTOD}_e = \dfrac{K_I^2}{m\sigma_Y E'}$.

It is possible to estimate CTOD from Eq. (19) provided that the applied load F is known. Stress intensity factor solution is available by using Eq. (9) (note that K_I is proportional to F and depends on geometry and flaw size) and a limit load solution is available by using Eqs. (5) and (6).

In the CDF method, fracture is considered to have occurred when J exceeds a material property value, CTOD_{mat}. This is related to experimentally obtained CTOD-R curves.

The CDF method described above is based on approaches within the ETM-ETM ´95 /17/. The routes FAD and CDF represent two different calculation methodologies, but the underlying principles remain the same. In spite of the differences that exist between these two methodological lines, FAD and CDF, both share the same concept, comparison between the applied stress and the materials resistance on a local scale. In spite of this, it is possible to combine both routes on the same component or specimen to predict initiation of stable crack growth and maximum load.

EXPERIMENTAL VALIDATION

The SINTAP method has been validated using experimental data of CTOD fracture toughness testing. As mentioned above, the FAD route has been used to determine the applied load for stable crack growth initiation, whilst the CDF route was used for determining the maximum load. The resulting failure assessment curves for both types of specimen (B×B and B×2B) are given in Fig. 7. Construction of the failure assessment curves for over-matching was made using mechanical properties, listed in Tab. 1, and Eq. (15), with yield load F_{YM} calculated by Eq. (6).
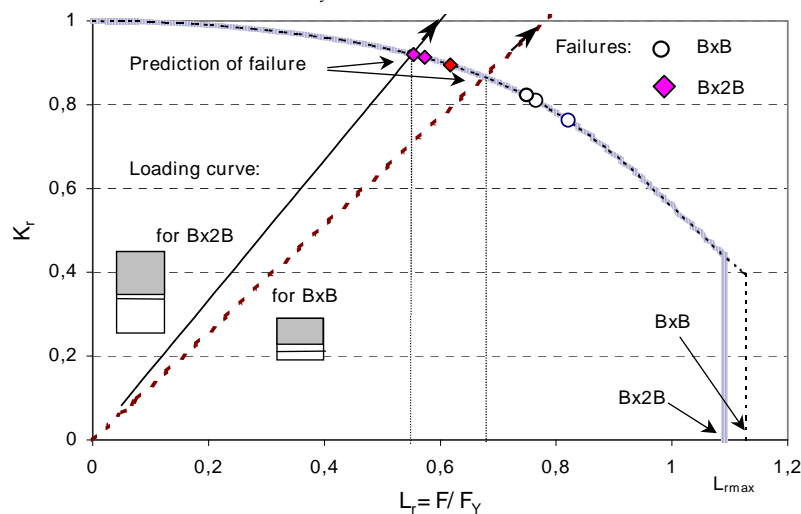

Figure 7. Determination of stable crack initiation load F_i, and comparison between experimentally obtained values and predicted values for two types of specimens (*B×B* and *B×2B*).
Slika 7. Određivanje opterećenja F_i za početak stabilnog rasta prsline, i poređenje eksperimentalno dobijenih vrednosti i predviđenih vrednosti za dva tipa epruveta (*B×B* i *B×2B*)

In spite of different specimen constraints, the loading path and L_r^{max} are different for each specimen type. Also, significant heterogamete of mechanical properties and simplification of the weld geometry leads to the observed differences between experimental and predicted values. The more accurate prediction is obtained for the B×2B specimen type. This confirmed that the assumption of relevant weld metal width was correct in the case of the through-the-thickness notched specimens.

In addition, the assumption for the initiation of stable crack growth occurrence under plane strain conditions in the mid-thickness of the specimen was confirmed. Figure 8 shows the CDF and CTOD-R curves of B×B and B×2B specimens. In spite of the fact that same weld metal was tested the CTOD-R curves are different for the same specimen type. It is obvious that different toughness values for crack initiation (CTODᵢ) were obtained. Different slopes on the CTOD-R curves were obtained, resulting from the different yielding and hardening ability of each specimen type. These differences in yielding and hardening behaviour are caused by heterogeneity of mechanical properties in the weld metal. Consequently, the tangency condition for each type of specimen and specimen with the same type of geometry is different. The differences in yielding and hardening are more significant for B×B specimens than for B×2B specimens, because the crack tip front in B×B specimens is mostly located in different types of microstructure in the same weld metal. Also, it is obvious that the B×B specimens have a lower constraint than B×2B specimens, as indicated by the higher slope of CTOD-R and CDF curves for B×B specimens. However, it is possible to determine the load for stable crack growth initiation and the maximum load using both route for each specimen type. Figure 9 shows good correlation between predicted and experimentally measured loads of stable crack growth initiation (by FAD) and maximum loads (by CDF). Less scatter is obtained by the CDF route than by FAD route for prediction maximum load and load for stable crack growth initiation.
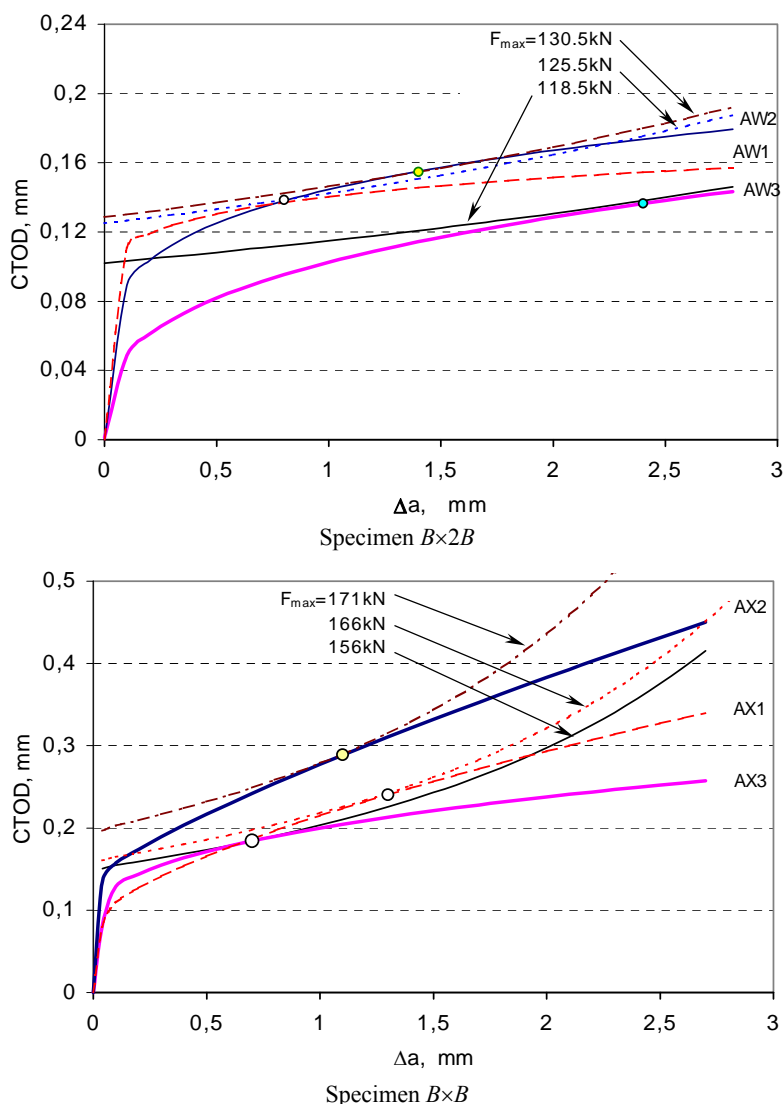

Specimen B×2B

Specimen B×B

Figure 8. Maximum loads predicted by use of the CDF route.
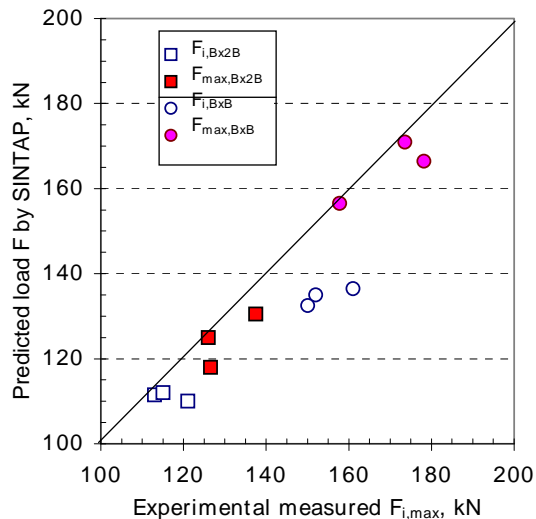Slika 8. Maksimalno opterećenje predviđeno postupkom CDF

Figure 9. Comparison between experimental and predicted values
of stable crack growth initiation load and maximum load.
Slika 9. Poređenje eksperimentalnih i predviđenih vrednosti opte-
rećenja početka stabilnog rasta prsline i maksimalnog opterećenja

CONCLUSION

The performed CTOD tests have shown a significant scatter of fracture behaviour (regarding crack initiation and maximum load) for high strength steel mis-matched weld,

even when the same specimens with the same position of notch were tested.

The reasons for the scatter in fracture toughness parameters result from different microstructures in the weld metal, and arises as a consequence of anisotropy weld metal behaviour.

Therefore, to correctly determine the fracture behaviour and range of fracture toughness parameters, it is necessary to test many CTOD specimens with the same geometry and same notch position.

The significance of mechanical anisotropy and deviation in the geometry of the welded metal gap require consideration of:

– minimum width of weld metal for the through-the-thickness notched specimens;
– current width of welded metal for the surface notched specimens;
– using plane strain condition in SINTAP analysis.

The assessment performed for high strength mismatched welds using the SINTAP procedure has shown that, in spite of heterogeneity and scatter of fracture behaviour, it is possible to predict correctly the stable crack growth initiation load and the maximum load for each type of specimens tested.

REFERENCES

1. Gubeljak, N., The effect of strength mis-match on welded joint fracture behaviour, dissertation, University of Maribor, Maribor, 1998.
2. R6: Assessment of the integrity of structures containing defects, Nuclear electric procedure R/H/R6, Revision 3, 1998.
3. Gilles, Ph., Franco, Ch., *A new J estimation scheme for cracks in mis-matched welds – the ARMS method*, Proc. Int. Symp. Mis-Match 93, ESIS 17. Mechanical Engineering Publications, London, 661-683, 1994.
4. WES 2805-1997, Japan Welding Engineering Society Standard, Method of Assessment for flaws in fusion welded joints with respect to brittle fracture and fatigue crack growth, The Japan Welding Engineering Society, 1997.
5. Schwalbe, K.-H., et al., EFAM ETM 97: The ETM method for assessing the significance of crack-like defect in Engineering Structures, GKSS 98/E/6, GKSS Research Centre, Geesthacht, Germany, 1998.
6. SINTAP Procedure, Final version: November 1999.
7. Koçak, M., et al., *Comparison of fatigue pre-cracking methods for fracture toughness testing of weldments: Local Compression and Step-Wise High Ratio*, Conference Welding-90, 1990.
8. BS 7448: Part 2: 1997: Fracture mechanics toughness tests, Part 2. Method for determination of K_{Ic}, critical CTOD and critical J values of welds in metallic materials, British Standards Institution, London, 1997.
9. GKSS (1992): Displacement Gauge System for Applications in Fracture, Mech, Patent Publication, Geesthach,1992.

10. Fairchild, D.P. et al., *Philosophy and Technique for Assessing HAZ Toughness of Structural Steels Prior to Steel Production*, Paper OMAE-88-910, 7th Int. Conf. on Offshore Mechanics and Arctic Eng., Houston, TX, 1988.
11. Johnson, H.H., Materials Research and Standards, 5, 442, 1965.
12. ASTM E 1290-93: Standard test method for crack tip opening displacement (CTOD) fracture toughness measurement, American Society for Testing and Materials, Philadelphia, 1993.
13. Schwalbe, K-H. et al., The GKSS test procedure for determining the fracture behaviour of materials, EFAM GTP 94, Geesthacht, 1994.
14. Gubeljak, N., *Estimation of Lower Bound Toughness in Strength Miss-Match Welded Joints*, Welding in the World, Vol. 43, No. 6, 1999.
15. Schwalbe, K.-H. et al., EFAM ETM 97 – The ETM method for assessing the significance of crack-like defects in engineering structures, comprising the versions ETM 97/1 and ETM 97/2.
16. Kirk, M.T., Wang, Y.-Y., *Wide range CTOD extermination formulae for SE(B) specimens*, Fracture Mechanics, Vol. 26, ASTM STP 1256, W.G. Reuther, J.H. Underwood and J.C. Newman, Jr. Eds., ASTM, Philadelphia, 1995.
17. Schwalbe, K-H. et al., EFAM ETM-MM 96–The ETM Method for assessing the significance of crack-like defects in joints with mechanical heterogeneity (strength mismatch), GKSS 97/E/9.